A non-olfactory shark adenosine receptor activates CFTR with unique pharmacology and structural features

Sumeet Bhanot, Gabriele Hemminger, Cole L. Martin, Stephen G. Aller and John N. Forrest Jr.

Renal Section, Department of Medicine, Yale University School of Medicine, New Haven CT 06510
The Mount Desert Island Biological Laboratory, Salisbury Cove, ME 04672
The Department of Pharmacology & Toxicology, University of Alabama at Birmingham, Birmingham, AL 35205

Running Head: Characterization of a novel adenosine receptor (A_0) from the shark rectal gland (*Squalus acanthias*)

Corresponding Authors: Stephen G. Aller, Department of Pharmacology & Toxicology, University of Birmingham at Alabama, Birmingham, AL 35205, sgaller@uab.edu
and John N. Forrest Jr., Department of Medicine, Yale University School of Medicine, 367 Cedar St., New Haven CT 06510, john.forrest@yale.edu

Abstract

Adenosine receptors (ADORs) are G-protein coupled purinoceptors that have several functions including regulation of chloride secretion via CFTR in human airway and kidney. We cloned an ADOR from *Squalus acanthias* (shark) that likely regulates CFTR in the rectal gland. Phylogenic- and expression- analyses indicate that elasmobranch ADORs are non-olfactory, and appear to represent extant predecessors of mammalian ADORs. We therefore designate the shark ADOR as the A_0 receptor. We co-expressed A_0 with CFTR in *Xenopus laevis* oocytes and characterized the coupling of A_0 to the chloride channel. Two electrode voltage clamping was performed and current-voltage (I-V) responses were recorded to monitor CFTR status. Only in A_0- and CFTR- co-injected oocytes did adenosine analogs produce a significant concentration-dependent activation of CFTR consistent with its electrophysiological signature. A pharmacological profile for A_0 was obtained for ADOR agonists and antagonists that differed markedly from all mammalian ADOR subtypes (agonists: R-PIA > S-PIA > CGS21680 > CPA > 2ClADO > CV1808 = DPMA > NECA) and (antagonists: DPCPX > PD115199 > 8PT > CGC > CGS15943). Structures of human ADORs permitted a high-confidence homology model of the shark A_0 core which revealed unique structural features of ancestral receptors. We conclude: (1) A_0 is a novel and unique adenosine receptor ancestor by functional and structural criteria; (2) A_0 likely activates CFTR *in vivo* and this receptor activates CFTR in oocytes indicating an evolutionary coupling between ADORs and chloride secretion; and (3) A_0 appears to be a non-olfactory evolutionary ancestor of all four mammalian ADOR subtypes.

Keywords

Adenosine receptor, molecular evolution, shark, structural biology, CFTR, chloride secretion

Significance Statement

We have cloned and characterized an ancient adenosine receptor from sharks that is unlikely to be olfactory in function. The shark receptor, which we designate as A_0, has a unique pharmacological profile, characteristic structural features, and is also highly likely to be the dominant ADOR regulator of the shark ancient ortholog of the Cystic Fibrosis chloride channel, called CFTR.

Introduction

Two broad classes of purinoceptors, P_1 & P_2, recognize and bind adenosine-based nucleosides and nucleotides, and can be distinguished by two anti-parallel pharmacological profiles (P_1: Adenosine > AMP > ADP > ATP & P_2: ATP > ADP > AMP > Adenosine) (1). Receptors specific for adenosine (ADORs) are divided into four non-olfactory subtypes including A_1, A_{2a}, A_{2b} & A_3, which couple to $G_{o,i(1-3)}$, G_s, G_s and $G_{i(2,3),q\text{-like}}$ G proteins, respectively (2-7). Typically, all ADORs modulate the activity of at least one of a number of different isoforms of adenylyl cyclase through the coupling to a G protein. The A_1 ADOR can also modulate other effector systems, namely potassium channels, calcium channels, phospholipase A and C (7).

One major unifying theme in the function of ADORs in mammals appears to be a feedback mechanism to either curb metabolic activity of the cell or to oppositely vasodilate for increasing oxygen supply and meet higher metabolic demand (8). Relatedly, in sharks, which evolved prior to any land-based vertebrate, low concentrations of adenosine released from metabolic activity by the highly active shark rectal gland of *Squalus acanthias*, serve as an autocoid feedback inhibitor to slow ion transport (9). Curiously, high concentrations of adenosine (~10 μM) increased ion transport activity at both the apical- and basolateral-membranes, and stimulated chloride secretion in rectal gland via the shark ortholog of the Cystic Fibrosis transmembrane Conductance Regulator (CFTR) (10,11). Shark CFTR is an impressive 70% identical to human CFTR at the amino acid residue sequence level (12), and an ancient evolutionary link in ADOR signaling of CFTR activity in both fish and mammals is now well established.

The four main ADOR subtypes (A_1, A_{2a}, A_{2b} & A_3), first identified in many different mammals and now observed in the genomes of birds, reptiles, amphibians and fish, can be distinguished at phylogenetic- and pharmacological levels. For the A_1 receptor, the adenosine analogs CPA and R-PIA are the most potent, while CV1808 and CGS21680 are weaker agonists. For A_{2a}, NECA, CV1808, and CGS21680 are the most potent agonists, and CPA is less potent. The A_{2b} receptor subtype responds with high potency to NECA but exhibits little or no response to CV1808 and CGS21680. A fifth ADOR subtype, designated A2c, was more recently identified and was shown to be an olfactory ADOR that allows fish to sense adenosine released into the water by potential prey (13).

We sought to examine ADORs in *Squalus acanthias* and we identified a single receptor with highest expression in the rectal gland and stomach, but very low levels in brain and other tissues. Phylogenetic analysis shows that the *Squalus acanthias* ADOR, as well as putative ADORs identified by genome sequencing from other sharks, amphibians and reptiles, form a separate clade that is distinct from the other five ADOR subtypes. We used the *Xenopus laevis* oocyte system to co-express the *Squalus acanthias* ADOR with CFTR to demonstrate the coupling of receptor to chloride channel. Co-injected oocytes revealed a pharmacological profile of *Squalus acanthias* ADOR that is unique from all four major subtypes of ADORs. We argue that the *Squalus acanthias* ADOR is not olfactory and that the clade containing the elasmobranch ADORs is ancestral to the four major subtypes. We therefore designated the shark ADOR as A_0-ADOR, and characterize this ancestral receptor here including novel structural features revealed by three-dimensional atomic homology modeling.

Materials and Methods

Molecular Biology

Tissues were obtained from male dogfish sharks, *Squalus acanthias*, weighing 2-4 kg, which were caught by gill nets in Frenchman's Bay, ME, and kept in marine live cars until use, usually within 3 days of capture. One male dogfish shark was killed by pithing the spinal cord. Details describing the molecular biology (preparation of total RNA from shark tissue, degenerate PCR, library screening, RACE PCR, Northern blot, qRT-PCR and electrophysiology in oocytes) are presented in the supplementary material (see supplementary figs. S1-S5, https://www.biorxiv.org/content/biorxiv/early/2020/11/02/2020.11.01.363762/DC1/embed/media-1.pdf?download=true). Human CFTR was obtained from Dr. Carol Semrad in the pKS-βglobin-CFTR-polyAC plasmid and human adenosine receptors were provided by Dr. Joel Linden. Capped messenger RNA for all receptors was synthesized from linearized plasmid templates using the Ambion mMessage mMachine T7 *in vitro* transcription kit according to the manufacturer's protocol.

To retrieve putative adenosine receptor coding sequences with good representation from mammals, birds, reptiles, amphibians and fish, multiple database searches were carried out using the NCBI BlastP Server against the full nonredundant dataset. To find potential ancestral receptor sequences, additional searches using shark A_0 sequence were performed excluding the Mammalia taxid (40674). Global alignments were performed using the Clustal method (14) within the Lasergene software package (DNASTAR, Inc) and similar results were obtained using the implementation of Clustal Omega (15) in the EMBOSS package (16) and standard parameters (17). Alignments for phylogenetic analyses including the production of the phylogenetic tree in figure 1 were conducted with MEGA7 (18).

Xenopus laevis expression system

Adult female *Xenopus laevis* were obtained from Nasco and Xenopus 1, and housed in the animal care facilities at Yale University. Surgeries to harvest oocytes were performed 4-7 days prior to experiments according to a protocol approved by the Yale Animal Care Committee. Injection pipets pulled on a Sachs-Flaming Micropipette puller Model PC-84, using Drummond 210/310/510 glass pipettes were beveled to a tip diameter of 10-15 µm. The pipettes were back-filled with mineral oil and attached to a Drummond microinjector, in preparation for cRNA aspiration and oocyte injection. Oocytes were injected with 50 nl (~15 ng) of cRNA encoding shark A_0- or human A_1, A_{2a}, A_{2b}, or A_3 receptors and 5-10 ng of human CFTR, and subsequently incubated for 3-5 days at 18-20 °C before experiments.

Oocytes were prepared for two electrode voltage clamping by inserting two 0.6-0.9 MΩ, 3 M KCl filled Ag electrodes, pulled on a Sachs-Flaming micro-pipet puller model PC-84, using borosilicated glass obtained from Sutter Instrument (BF120-69-10). Oocytes were perifused with frog Ringer's, FR, (98 mM NaCl, 2 mM KCl, 1.8 mM $CaCl_2$, 1 mM $MgCl_2$ and 5 mM HEPES. Adjusted to pH 7.4), which was also used in the preparation of solutions for the pharmacological agents tested. Oocytes were voltage clamped using the Dagan TEV-200 amplifier along with the Dagan LM-12 Lab Interface, on a PC computer running pClamp Version 5.5 software. The Soltec 1242 plotter was used to acquire the data. Oocytes were clamped at -60 mV and the current was measured as a function of time. Moreover, frequent voltage pulses (-120mV to +60mV) were performed to determine the current-voltage (I-V) relationship at any given timepoint. Data were corrected for any capacitive current incurred due to the voltage pulses. Inconclusive data were obtained with the human A_{2a} and A_3 receptors, which presumably do not couple efficiently to frog G proteins or the proper adenylyl

143 cyclase(s) for CFTR activation, and were omitted from the analysis.
144 Data analysis was performed using Microsoft Excel. Some of the data were analyzed using an
145 Excel macro provided by the lab of Dr. David Dawson, which allowed the subtraction of the capacitive
146 current from the current voltage relationship, incurred during the voltage pulses. Statistical analysis was
147 limited to standard deviation performed on the concentration response of the shark A_0 receptor.
148
149 **Homology model of the shark A_0**
150 At the time of this writing there were 48 high-resolution structures of adenosine receptors in
151 the Protein Data Bank (PDB) as determined by either x-ray crystallography or cryo-electron
152 microscopy. All structures are human in origin and only two of the four known subtypes were
153 represented, A_{2a} (n=45) and A_1 (n=3). We chose a small subset for consideration as templates for
154 homology modeling of the shark A_0 receptor: A_{2a} with adenosine bound (PDB code 2ydv) (19), A_1
155 with adenosine (6d9h) (20), A_{2a} with N-ethyl-5'-carboxamido adenosine, NECA (6gdg) (21), and
156 A_{2a} with CGS21680 (4ug2) (22). Primary amino acid sequence alignments between shark A_0
157 sequence and the selected subset were performed using NCBI Cobalt (23). Amino acid sequences
158 present in the human receptors but not present in shark A_0 were removed (see full alignment
159 between shark A_0 and human A_{2a} in supplementary fig. S6,
160 https://www.biorxiv.org/content/biorxiv/early/2020/11/02/2020.11.01.363762/DC1/embed/media-1.pdf?download=true).
161 The human A_{2a} receptor appeared to be a sufficiently good template for A_0 modeling as it shares
162 45% identical amino acid sequence with A_0 and exhibited an NCBI Cobalt 3-bit amino acid
163 chemical similarity of 81% after removing disordered sequences from the A_{2a} structure, and after
164 removing sequences present in either receptor but not the other (supplementary fig S7,
165 https://www.biorxiv.org/content/biorxiv/early/2020/11/02/2020.11.01.363762/DC1/embed/media-1.pdf?download=true).
166 Using the A_{2a} x-ray crystal structure template (PDB code 2ydv), A_{2a} insertion sequences were
167 removed and mutagenesis to A_0 was performed with scripts written in perl and PyMOL version
168 2.0.6 (Schrödinger, LLC). Two short amino acid sequences of shark A_0 that are not present in the
169 human receptors (i.e. A_0-Arg95 and A_0-Asn228-Ser230), were inserted into the 3-dimensional
170 model using Coot version 0.8.9 (24) and model minimization/regularization. Refinements using
171 phenix (25) of A_0 against A_{2a} dataset (PDB code 2ydv) were performed by replacing the human
172 receptor with the shark starting model. Three rounds of rigid body, XYZ-reciprocal space and B-
173 factor refinement were performed including secondary-structure restrains and
174 Ramachandran/rotamer optimization, all with resolution cutoff set to 4.0 Å resolution.
175 Parameterization of the R-PIA ligand was accomplished using phenix (25) starting with the
176 Simplified Molecular-Input Line-Entry System (SMILES) string for the ligand (26):
177 C[C@H](Cc1ccccc1)Nc2ncnc3n(cnc23)[C@@H]4O[C@H](CO)[C@@H](O)[C@H]4O
178 The position of the lipid bilayer was predicted based on the location of conserved aromatic amino
179 acids known to interact with lipid head groups spaced ~35 Å apart (27).
180
181 **Results**
182 **Identification of shark A_0 ADOR**
183 Since the *Squalus acanthias* genome is not yet available and there is some uncertainty associated
184 with the search for *bona fide* protein-coding sequences from genomic data, we sought to clone shark
185 adenosine receptors using reverse-transcription procedures from mRNA/cDNA prepared from shark
186 tissues. PCR of shark rectal gland cDNA using degenerate primers to conserved regions of
187 transmembrane domains 5 and 7 of previously cloned ADORs yielded a single 352 bp product (see

188 supplementary fig. S1). The translated amino acid sequence of this fragment (P-SH12) had highest
189 homology to ADORs that was only 39-45% identical to the human receptor sub-types (A_1, A_{2a}, A_{2b}
190 and A_3). Northern blot and quantitative RT-PCR (qRT-PCR) revealed strongest expression of the
191 putative shark ADOR in the rectal gland and stomach with weak levels in other tissues including the
192 brain (supplementary figs. S2 and S3). To control for the quality of cDNA template used in the qRT-
193 PCR experiments, shark CFTR was amplified from the same cDNA templates prepared from the various
194 shark tissues. Results showed abundant CFTR expression in rectal gland, intestine, brain and testis
195 (supplementary fig. S4).
196 Screening of a shark rectal gland cDNA library using ^{32}P-labeled P-SH12 yielded more
197 nucleotide sequence from a single putative ADOR and allowed the design of primers for Rapid
198 Amplification of cDNA Ends-PCR (RACE-PCR). Extensive rounds of both cDNA library screening and
199 RACE-PCR using total RNA from shark rectal gland revealed only a single putative ADOR entity
200 which we designate here as the shark A_0 receptor (for details see supplementary material).
201 Hydropathy analysis of the putative shark A_0 ADOR amino acid sequence revealed seven
202 predicted transmembrane regions and a predicted extracellular orientation of the N-terminus that was
203 consistent with all known G protein-coupled receptors (see supplementary fig. S5). Phylogenetic
204 analysis of known- and putative- ADORs revealed an ancestral branch that included dogfish shark A_0
205 and other putative ADORs from non-mammalian species that are distinct from the recently discovered
206 olfactory ADORs (Wakisaka et al. 2017; figure 1). Ancestral olfactory- and non-olfactory receptors
207 could be distinguished from the four specialized mammalian subtypes (i.e. A_1, A_{2a}, A_{2b} and A_3) as
208 having an abbreviated second extracellular loop (ECL2) at 9 amino acid (aa) residues (supplementary
209 fig. S8, https://www.biorxiv.org/content/biorxiv/early/2020/11/02/2020.11.01.363762/DC1/embed/media-
210 1.pdf?download=true). ECL2 of A_1 is elongated by 4-17 aa (n=42 receptor species examined), ECL2 of
211 A_{2a} is elongated by 8-14 aa (n=22), ECL2 of A_{2b} is elongated by 10-19 aa (n=28) and ECL2 of A_3 is
212 elongated by 1-7 aa (n=18, see supplementary fig. S9,
213 https://www.biorxiv.org/content/biorxiv/early/2020/11/02/2020.11.01.363762/DC1/embed/media-1.pdf?download=true).
214 Assuming mutagenesis rates of all adenosine receptors are similar amongst species, we interpret the
215 phylogram to indicate that the elasmobranch A_0 ADOR belongs to an evolutionary ancestral branch of
216 the specialized adenosine receptor subtypes. We next surmised that shark A_0 is responsive to adenosine
217 analogs with potentially unique properties compared to known receptor subtypes, and we sought to test
218 this hypothesis using functional and pharmacological characterization in *Xenopus laevis* oocytes.
219
220 **CFTR expression**
221 Expression studies were conducted in oocytes co-injected with human CFTR and shark A_0
222 cRNA, and current-voltage (I-V) relationships were determined by imposing voltage pulses (-120 mV to
223 +60 mV) and measuring the clamping current. Expression of CFTR was determined by the use of
224 forskolin, a well-known activator of adenylyl cyclase that increases intracellular cAMP levels and
225 activates CFTR by phosphorylation of the R-domain by a cAMP dependent protein kinase A (Dulhanty
226 and Riordan 1994). Figure 2 illustrates the I-V relationships of a single representative experiment on an
227 oocyte 3 days after co-injection. Addition of 5 μM forskolin produced an increase in conductance
228 (increase in the slope of the I-V relationship) from the basal level, an increase in the magnitude of the
229 clamping current at -60 mV from -76 nA to -563 nA, and a rightward shift in the reversal potential to -
230 29.4 ± 0.75 mV (n=3 I-V ramps ± SD) from a basal value of -38.0 ± 3.8 mV (n=5 ramps ± SD). This
231 negative, non-rectifying current with a reversal potential close to that of Cl^- (Cl^-_{rev} = ~ -30 mV) has the
232 electrophysiological characteristics of a CFTR Cl^- current. Furthermore, this response was sensitive to

233 300 μM glibenclamide, an inhibitor of the CFTR Cl^- channel (28) (n=1, data not shown). The response
234 to forskolin was also inhibited by the PKA antagonist H-89 (25 μM, n=3) in oocytes injected with
235 human CFTR cRNA (data not shown), suggesting that CFTR is activated by a cAMP dependent protein
236 kinase (PKA) in this system. To confirm, we measured total cAMP in oocytes expressing the shark A_0
237 receptor and observed an increase in total cAMP that paralleled the order of agonist potency we
238 observed in electrophysiology experiments (see supplementary fig. S10). The negative, non-rectifying
239 CFTR current was absent in un-injected- and water injected- oocytes (n=4) under identical conditions,
240 and were reproducible both in the same oocyte and in all oocytes injected with human CFTR cRNA.
241 These data established expression of CFTR in our system.
242 Addition of 10 μM 2-chloroadenosine in the representative oocyte (figure 2) also
243 produced an increase in total current by a similar non-rectifying negative current of the
244 magnitude ~ -500 nA and a reversal potential of approximately -30.5 ± 0.28 mV (n=3 ramps ±
245 SD). This response was reversibly inhibited by 10 μM DPCPX, an adenosine receptor
246 antagonist, where the clamping current at -60 mV was ~ -90 nA with a reversal potential of -
247 39.4 ± 4.8 mV (n=3 ramps ± SD), both of which are reminiscent of the basal state (figure 2).
248 This response suggested that the expression and stimulation of the shark A_0 receptor is
249 associated with an increase in Cl^- current which has characteristics consistent with CFTR $C1^-$
250 currents. Our results also established a coupling of the shark A_0 adenosine receptor and human
251 CFTR in the *Xenopus* oocyte expression system.
252
253 **Pharmacological characterization of shark A_0**
254 Determination of the pharmacological profiles of adenosine receptor agonists and
255 antagonists in the oocyte necessitated the development of protocols in the *Xenopus laevis* oocyte
256 expression system. We first compared three agonists in a series of identical experiments to provide
257 quantitative data for statistical analysis. We then developed a second protocol to determine a
258 relative response to a larger number of agonists and antagonists to provide a more comprehensive
259 profile for comparison with other receptor profiles in the literature.
260
261 **<u>Quantitative concentration response to agonists</u>**
262 Based on preliminary data, NECA, 2-chloroadenosine (2ClAdo) and R-PIA were selected to
263 determine potency order in a quantitative manner. The concentration response to each agonist was
264 measured as in the representative experiment shown in figure 3. Oocytes were first stimulated with
265 sub-maximal 5 μM forskolin, and subsequently brought to a basal state with frog Ringer's (FR).
266 The forskolin concentration was chosen to avoid desensitization of the adenylyl cyclase/CFTR
267 pathway since each oocyte was stimulated multiple times by forskolin and adenosine analogs. Next,
268 the oocytes were exposed to increasing concentrations of NECA (0.01 μM, 0.1 μM, 1 μM & 10
269 μM), each incremental concentration of the agonist was added once the response to the prior
270 concentration had peaked (n=3). This sequence was followed by an identical protocol for 2-
271 chloroadenosine (n=3) and R-PIA (n=6). Variation in the sequence of the agonists tested gave
272 similar results.
273 The initial 5μM forskolin response was used as an internal control (comparison of the
274 agonist response to forskolin) in these studies because of the variability of the expression of CFTR
275 secondary to imprecision in injection of RNA, inter-oocyte variability in CFTR expression and
276 inter-frog and intra- frog variability in the quality of the oocytes due to environmental factors. Data
277 were normalized to the response to 5μM forskolin preceding each concentration response.

278 Results from the concentration response experiments are summarized in figure 4. The peak
279 normalized stimulation of the control oocytes (injected with human CFTR cRNA only) at 10 μM of
280 NECA, 2-chloroadenosine and R-PIA are -0.01%, 0.04% and 0.03% respectively (normalized to 5
281 μM forskolin responses, n=2 each, with mean±SD of 191±26 nA, 231±27 nA and 295±96 nA,
282 respectively), showing very poor coupling of any endogenous oocyte adenosine receptor to human
283 CFTR. The responses of oocytes injected with human CFTR and shark A_0 cRNA, at concentrations
284 of 0.01 μM of NECA, 2-chloroadenosine and R-PIA, and 0.1 μM NECA and 2-chloroadenosine
285 were not significantly different from un-injected controls ($p>0.05$). The response to R-PIA at 0.1
286 μM (55.6%) was greater than NECA and 2-chloroadenosine (2.7% and 4.2% respectively). At an
287 agonist concentration of 1 μM the differences between the three agonists NECA, 2-chloroadenosine
288 and R-PIA (13.0%, 35.1% and 196%, respectively) were appreciable and significant ($p<0.05$). The
289 response at 10 μM (66.5%, 151% and 210% respectively) were markedly different ($p<0.05$). The
290 probability values for determining a significant main effect for each of these observations were
291 obtained using an ANOVA. These data established the potency order of R-PIA>2- chloro-
292 adenosine>NECA for the shark A_0 adenosine receptor in *Xenopus laevis* oocytes.
293
294 **Qualitative profile for agonists and antagonists**
295 With the above profile established for the three agonists, a more extensive profile was
296 ascertained for 8 agonists (NECA, DPMA, CV1808, 2-chloroadenosine, CPA, S-PIA, CGS21680,
297 R-PIA) and 5 antagonists (CSC, 8PT, DPCPX, CGS15943, PD115199) to allow comparison with
298 profiles established for the presently cloned adenosine receptors. The analysis was carried out at an
299 agonist concentration of 1 μM and an antagonist concentration of 10 μM to optimize the analysis.
300 The protocol required oocyte perifusion with one agonist at 1 μM and substitution with a
301 second after stabilization of the signal. The responses were judged as either an increase, a decrease
302 or equivocal. The data were compiled into the agonist profile for the shark A_0 receptor of R-
303 PIA>S-PIA>CGS21680>CPA>2-chloroadenosine>CV1808=DPMA>NECA (n=7). Varying the
304 order of agonists produced highly consistent results, in that the profiles conducted in order of
305 increasing agonist potency were usually no different from profiles conducted in order of decreasing
306 agonist potency.
307 The antagonist order of potency was carried out using a similar protocol. Oocytes were
308 perifused with 1 μM R-PIA to generate a stable stimulated state, followed by perifusion with 1 μM R-
309 PIA and 10 μM of the various antagonists. The antagonist profile obtained for the shark A_0 receptor was
310 DPCPX>PD115199>8PT>CSC>CGS15943 (n=5). The relative potency order of agonists- and
311 antagonists- were determined qualitatively in 10 different oocytes including 186 pairwise comparisons
312 (please see supplementary tables S3,
313 https://www.biorxiv.org/content/biorxiv/early/2020/11/02/2020.11.01.363762/DC1/embed/media-1.pdf?download=true),
314 and 91% (n=169) of all pairwise observations agree with our final conclusion of potency order.
315
316 **Protocol validation using human ADORs**
317 The human A_1, A_{2a}, A_{2b} and A_3 receptors, obtained from the Linden lab at the University
318 of Virginia, were also examined in our oocyte system using the qualitative protocol to provide
319 validation for this form of analysis. Although four human ADORs were expressed in the oocyte,
320 reproducible profiles were obtained for two receptors, the human A_1 (agonist profile, n=3) and
321 human A_{2b} (agonist profile, n=4, antagonist profile, n=3) (table 1). The human A_1 and A_{2b}
322 receptor agonist profiles determined in oocytes are in excellent agreement with binding studies

323 and functional studies (see supplementary table S4,
324 https://www.biorxiv.org/content/biorxiv/early/2020/11/02/2020.11.01.363762/DC1/embed/media-1.pdf?download=true).
325 However, the A_{2b} antagonist profile shows an apparent discrepancy in the potency order of
326 CGS15943 and 8PT. This difference may be attributable to a cross species comparison (rat vs
327 human). Taken together, this data provides strong support for the validity of our protocols used in
328 pharmacological characterization of human- and shark- ADORs.
329
330 **Homology model of shark A_0**
331 Given the reasonable sequence homology of shark A_0 between ADORs that have been well-
332 characterized and for which structures are known (supplementary fig. S11,
333 https://www.biorxiv.org/content/biorxiv/early/2020/11/02/2020.11.01.363762/DC1/embed/media-1.pdf?download=true),
334 we conducted exploratory refinements of the A_0 starting homology model against the deposited
335 structure factors of the human A_{2a} x-ray crystal structure (PDB 2ydv), replacing the coordinates of
336 A_{2a} with A_0. Refinement was restricted to low-resolution (4.0 Å) to effectively down-weight the
337 contribution of mis-matched side chain sequences between the two species while providing a data-
338 driven constraint for backbone atoms and secondary structure. The resulting model exhibited good
339 protein Ramachandran- and side chain rotameric geometry (supplementary table S5,
340 https://www.biorxiv.org/content/biorxiv/early/2020/11/02/2020.11.01.363762/DC1/embed/media-1.pdf?download=true)
341 and had convincing secondary structure for the transmembrane helices and extramembrane
342 segments (figure 5). Both sequence alignments and the shark A_0 homology model revealed an
343 abbreviated extracellular loop 2 (ECL2) in ancestral receptors compared to the more specialized
344 subtypes. While it is not yet known what, if any, functional consequence arises from different
345 lengths of the ECL2 specifically, more than 30 ancestral receptors in the database have a minimized
346 ECL2 (supplementary fig. S8). Thus, it would seem that ECL2 of ancestral receptors is at the
347 minimum length necessary to maintain the structure and/or function of the adenosine receptor
348 architecture.
349
350 **Conserved Ligand-Receptor Interactions**
351 To explore the extent to which our homology model recapitulates known fundamental
352 interactions between ligand and receptor, we separately modeled adenosine (ADO), 2-
353 chloroadenosine and the most potent ligand in this work, R-phenyl-isopropyl adenosine (R-PIA),
354 into the A_0 binding pocket, conducted refinements and inspected the receptor-ligand interactions.
355 While we recognize there will be error in the process of homology modeling A_0 in the absence of
356 an actual structure, potential fundamental interactions between A_0 and ligands are well conserved
357 in the refined A_0 model compared to human ADOR structures (figure 6 and supplementary table
358 S6, https://www.biorxiv.org/content/biorxiv/early/2020/11/02/2020.11.01.363762/DC1/embed/media-
359 1.pdf?download=true).
360 Among the most important known interactions between receptor and ligand occur between
361 ADOR and the purine pharmacophore of adenosine- and adenosine analogs. The structures of
362 human A_{2a}- and A_1 reveal that an aromatic residue (F168 and F171, respectively), protrudes down
363 into the ligand binding pocket and contribute an intimate π-π stacking interaction with the purine
364 ring of adenosine (29). Our refined homology model of shark preserves this interaction
365 convincingly well, with the corresponding A_0 aromatic residue being F179 (figure 6). A second
366 critical interaction revealed by the structures of A_{2a}- and A_1 is a strong polar interaction, most
367 likely hydrogen bonding, between an asparagine residue (N253 and N254, respectively) and the N7

368 nitrogen and the amino group of C6 of the purine ring. The corresponding A_0 asparagine is N267
369 (figure 6). These two interactions form the fundamental basis for recognizing the adenosine
370 pharmacophore and are invariant in all ADORs we have examined (see multiple sequence
371 alignments in supplementary figs. S12 and S13,
372 https://www.biorxiv.org/content/biorxiv/early/2020/11/02/2020.11.01.363762/DC1/embed/media-1.pdf?download=true). In
373 totality, nine amino acid residues in close proximity to the adenosine analog in our shark A_0
374 homology model are highly conserved in all known- and putative ADORs, including the ancestral
375 branch (see also supplementary table S6).
376
377 **Discussion**
378 **Co-expression of shark A_0 and human CFTR**
379 We successfully co-expressed the shark A_0 adenosine receptor with human CFTR in
380 *Xenopus laevis* oocytes, which, to our knowledge, represents the first heterologous co-expression of
381 any adenosine receptor with CFTR in the literature. Oocytes appear to be an ideal system to
382 characterize shark A_0, since neither frog ADORs nor frog CFTR appears to be active or coupled.
383 We coupled an adenosine receptor from an elasmobranch shark, a subclass of Chondrichthyes fish
384 with a temporal range dating back to at least the Devonian period (~419-360 million years ago), to
385 human CFTR using the endogenous G-proteins and cellular enzymes of the oocyte. Other
386 investigators have in the past exploited CFTR for co-expression studies, specifically with alpha 2-
387 adrenergic-, beta 2-adrenergic-, delta-opioid-, and the 5HT1A receptors ((30), (31)), however those
388 receptors were mammalian in origin, which would not be viewed nearly as long-lived as receptors
389 identified in the shark. A_0 function in oocytes suggests that the interaction between receptors and
390 frog G-proteins is maintained despite the ancestral properties and structural differences A_0 has with
391 respect to more specialized ADORs. This highlights a likely conservation of the interface between
392 G-proteins and receptors with which they interact, across species and through evolution. Our results
393 also emphasize the versatility and value of the *Xenopus laevis* expression system for studies of
394 GPCR molecular evolution.
395
396 **A_0 exhibits unique ADOR pharmacology**
397 We characterized the shark A_0 receptor in *Xenopus* oocytes using a novel protocol, in
398 contrast to previous studies using binding assays, *in vivo* functional studies and cAMP
399 measurements. To this end it was necessary to couple the shark A_0 with a reporter target protein, in
400 this case human CFTR, to permit measurement of expression by electrophysiology. The data from
401 these studies revealed a unique profile for the shark A_0 receptor. Table 2 summarizes the
402 comparison of the A_0 receptor to other adenosine receptors with respect to agonist potency.
403 The shark A_0 differs: 1) from A_1 in its potency order of 2ClAdo and NECA, 2) from A_{2a}
404 and A_{2b} which have the reverse potency order and 3) from A_3 in which the least potent shark A_0
405 agonist, NECA, and the most potent shark A_0 agonist, R-PIA, have equal potencies. Therefore, the
406 shark A_0 appears to have a unique agonist profile judging from the potency order of R-PIA >
407 2ClAdo > NECA.
408 Subsequent qualitative studies further established the unique nature of the shark A_0. Table 3
409 compares the pharmacological profile for the shark A_0 to mammalian A_1, A_{2a}, A_{2b} and A_3
410 adenosine receptor subtypes. Analysis reveals the A_1 specific agonist R-PIA is the most potent in
411 the shark, however the A_1 selective agonist CPA is of intermediate potency. While S-PIA and

412 CGS21680 are more potent in the shark A_0 than in the A_1 receptors. All of the above are
413 inconsistent with an A_1-like receptor profile for A_0.
414 The shark A_0 receptor is dissimilar to A_{2a} or A_{2b} with respect to its low potency to the A_2-
415 preferring agonist NECA. Furthermore, response of A_0 to S-PIA was unexpectedly high
416 considering that S-PIA is not relatively potent at A_1, A_{2a} or A_{2b} receptors. Interestingly, the A_{2a}
417 preferring agonist CGS21680 has relatively high potency in the shark A_0 profile, while CV1808,
418 also A_{2a} preferring, has a much lower potency in the profile. The shark A_0 profile bears little
419 resemblance to that of A_{2b} receptors especially with respect to the position of CGS21680, NECA,
420 R-PIA and S-PIA. Therefore, the shark A_0 resembles neither the A_{2a} nor the A_{2b} adenosine
421 receptors (table 3). Similarly, it is quite different from the known A_3 adenosine receptor profiles
422 (table 3), with low potency of NECA (intermediate potency in A_3), relatively high potency of
423 CGS21680 and 5-PIA (lower in the profile for A_3) and the large difference in potency of R-PIA
424 and NECA, which are of equal potency in the A_3 adenosine receptor profiles.
425 A comparison of the antagonist profiles yields similar results. Although the shark A_0
426 antagonist profile is reminiscent of the A_1 antagonist functional profile (table 3), when compared to
427 binding studies for the rat A_1 (supplementary table S7,
428 https://www.biorxiv.org/content/biorxiv/early/2020/11/02/2020.11.01.363762/DC1/embed/media-1.pdf?download=true),
429 the low potency of CGS15943 in the shark A_0 profile is striking. The relative potency of
430 CGS15943 is also incongruent with the rat A_{2a} and rat A_{2b} profiles (supplementary table S8,
431 https://www.biorxiv.org/content/biorxiv/early/2020/11/02/2020.11.01.363762/DC1/embed/media-1.pdf?download=true).
432 Moreover, the potency order of DPCPX>PDl15199 in the shark A_0, is reversed for A_{2a} receptors
433 and A_{2b} receptors. It is clear that shark A_0 also possess a unique antagonist profile.
434 In summary the agonist- and antagonist- profiles do not allow the classification of this
435 receptor into any known receptor subtype, providing functional evidence that A_0 is a unique
436 ADOR.
437
438 **A_0 is an extant ADOR ancestor**
439 Since the initial characterization of specialized adenosine receptor (ADOR) subtypes ~40
440 years ago, hundreds of ADORs have been identified. Many examples arise from genomic
441 sequencing but have not been characterized structurally or functionally. Phylogenetic analysis
442 shows that examples of specialized ADORs (i.e. A_1, A_{2a}, A_{2b} and A_3) are apparent throughout the
443 animal kingdom, including fish, amphibians, reptiles, birds and mammals. However, a separate
444 phylogenetic branch emerges from the analysis that contains ADORs in reptiles, amphibians and
445 fish, including the shark A_0 ADOR we have characterized here. Shark A_0, and the related
446 members on the branch, appear to be ancestral in nature. We draw this conclusion based on the
447 following: 1) amino acid sequence similarity of A_0 is roughly equally different from any specific
448 specialized subtype (A_1, A_{2a}, A_{2b} and A_3; see supplementary table S9,
449 https://www.biorxiv.org/content/biorxiv/early/2020/11/02/2020.11.01.363762/DC1/embed/media-1.pdf?download=true); 2)
450 the pharmacological profile of A_0 is significantly different from the profiles of any subtype; 3) A_0
451 belongs to a phylogenetic branch that is distinct from the branches formed by the other specialized
452 subtypes; and 4) ADOR members of the ancestor branch contains structural features unique only to
453 themselves, such as a minimal ECL2.
454 A_1, A_{2a}, A_{2b} and A_3 appear to be specialized for several reasons: 1) they have distinct and
455 consistent pharmacological profiles amongst their respective sub-branches; 2) they prefer to couple
456 to one G-protein alpha subunit (e.g. inhibitory $G_i\alpha$ or stimulatory $G_s\alpha$ on adenylyl cyclase activity),

457 and 3) they are abundant in birds and mammals which are thought to arrive later in evolution. The
458 latter point highlights an interesting observation: specialized ADORs are prevalent in mammals
459 which arrived more recently in evolution time-scales, but the ancestral receptors, including
460 olfactory- and non-olfactory ADORs, appear to have been lost in mammals.
461
462 **Conclusion**
463 We have cloned, expressed and characterized an adenosine receptor (A_0) from the dogfish
464 shark (*Squalus acanthias*) that exhibits novel pharmacology compared to all known subtypes (A_1,
465 A_{2a}, A_{2b} and A_3). A_0 and its closest relatives form a distinct ancestral phylogenetic branch from
466 the known subtypes and do not appear have representation in birds or mammals. All ancestral
467 ADORs appear to have distinguishing structural elements, such as a minimally short extracellular
468 loop 2. Shark A_0 expression is strong in rectal gland where it likely regulates chloride secretion but
469 its expression is weak in brain, allowing us to conclude that is not olfactory in primary function. A
470 non-olfactory ancestral branch of ADORs, including A_0 from elasmobranchs, amphibians, and
471 reptiles is now apparent from the wealth of genomic sequencing data.
472 In contrast to the recently identified olfactory ADOR (A2c) found exclusively in fish (13),
473 A_0 was cloned from the shark rectal gland, a non-olfactory epithelial organ known for diverse
474 GPCR-mediated regulation of chloride secretion via the CFTR chloride channel (32). Shark CFTR
475 is more than 70% identical to human CFTR, and ADOR regulation of CFTR in sharks and
476 mammals is well described (33,34). Taken together, a long-standing evolutionary functional
477 coupling between ADORs and CFTR-mediated chloride secretion in epithelial tissues is evident,
478 and the elasmobranch A_0 receptor emerges as a non-olfactory extant ancestor of specialized ADOR
479 subtypes that most likely regulates CFTR in the shark.
480
481

482 **Acknowledgements**
483 We wish to thank Drs. Stephanie Halene and Kristina Lübbe for their important
484 contributions toward the manuscript. This work was supported by a Howard Hughes Medical Institute
485 Grant to SB, internal UAB funding to SGA, and by NIH grants R01 DK034208, NIEHS P30 ES003828
486 and NSF grant DBI-0453391 to JNF.
487
488 **Data Availability**
489 We agree to deposit the shark adenosine receptor nucleotide sequence to public repositories
490 (NCBI) or make it available upon request.

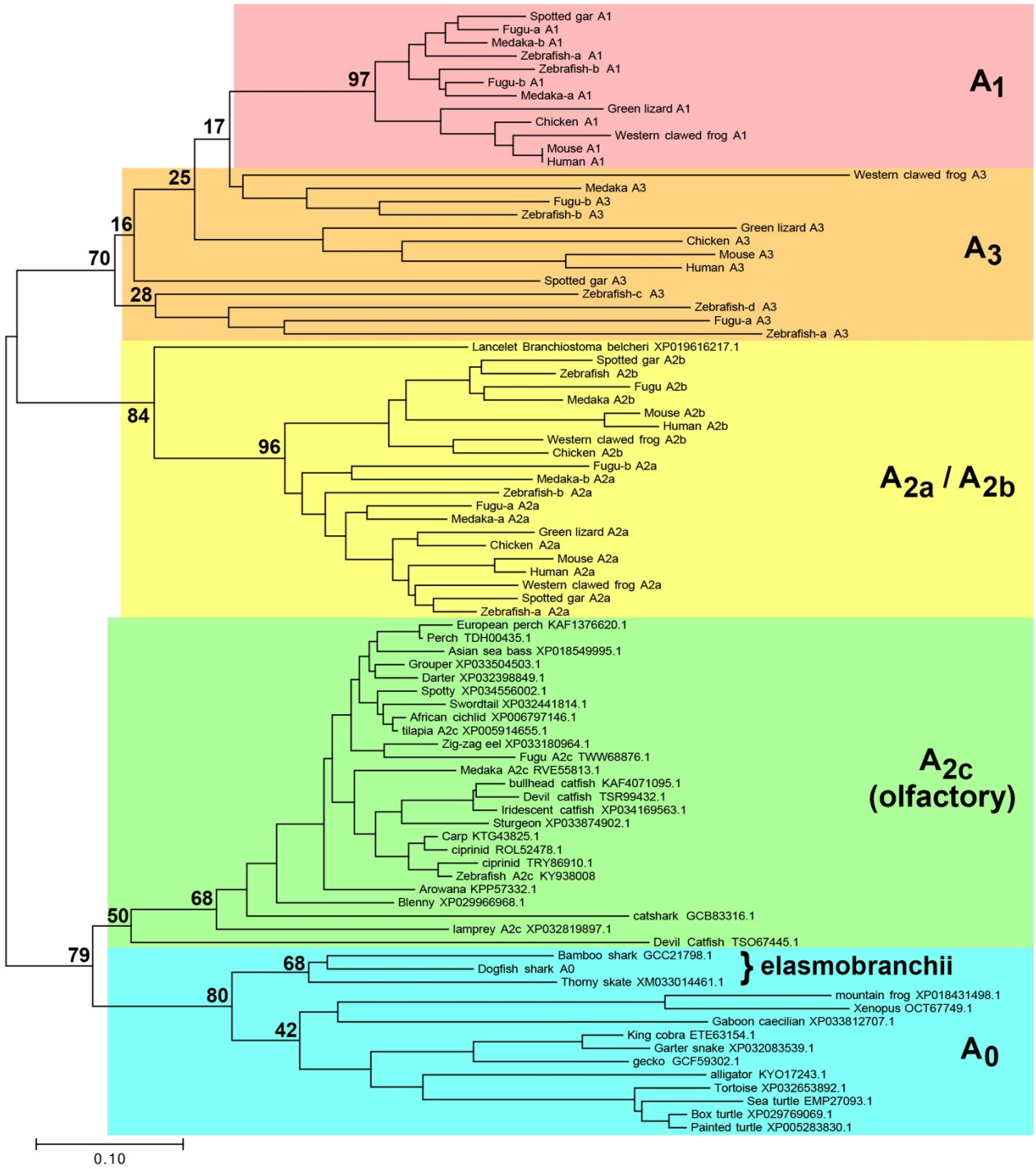

Figure 1. Phylogenetic relationships of ADOR taxa. Evolutionary history is inferred using the Neighbor-Joining method (35). The optimal tree is drawn to scale, with branch lengths in the same units as those of the evolutionary distances used to infer the tree. Distances were calculated using the Poisson correction method (36) and are in the units of the number of amino acids substitutions per site. A_1, A_{2a}, A_{2b}, A_3 and olfactory (A_{2c}) ADORs shown in Wakisaka, et al. 2017 are shown using the same names as in the paper. The first characterized A2c (Zebrafish, KY938008) by Wakisaka et al. is also shown in the figure. Additional putative ADORs found in this work are shown by species and Accession. The percentage of replicate trees in which the associated taxa clustered together in the bootstrap test using 500 replicates (Felsenstein 1985) are shown at selected branchpoints. Analyses were conducted using MEGA7 (Kumar, et al, 2016) using only full-length sequences for all receptors.

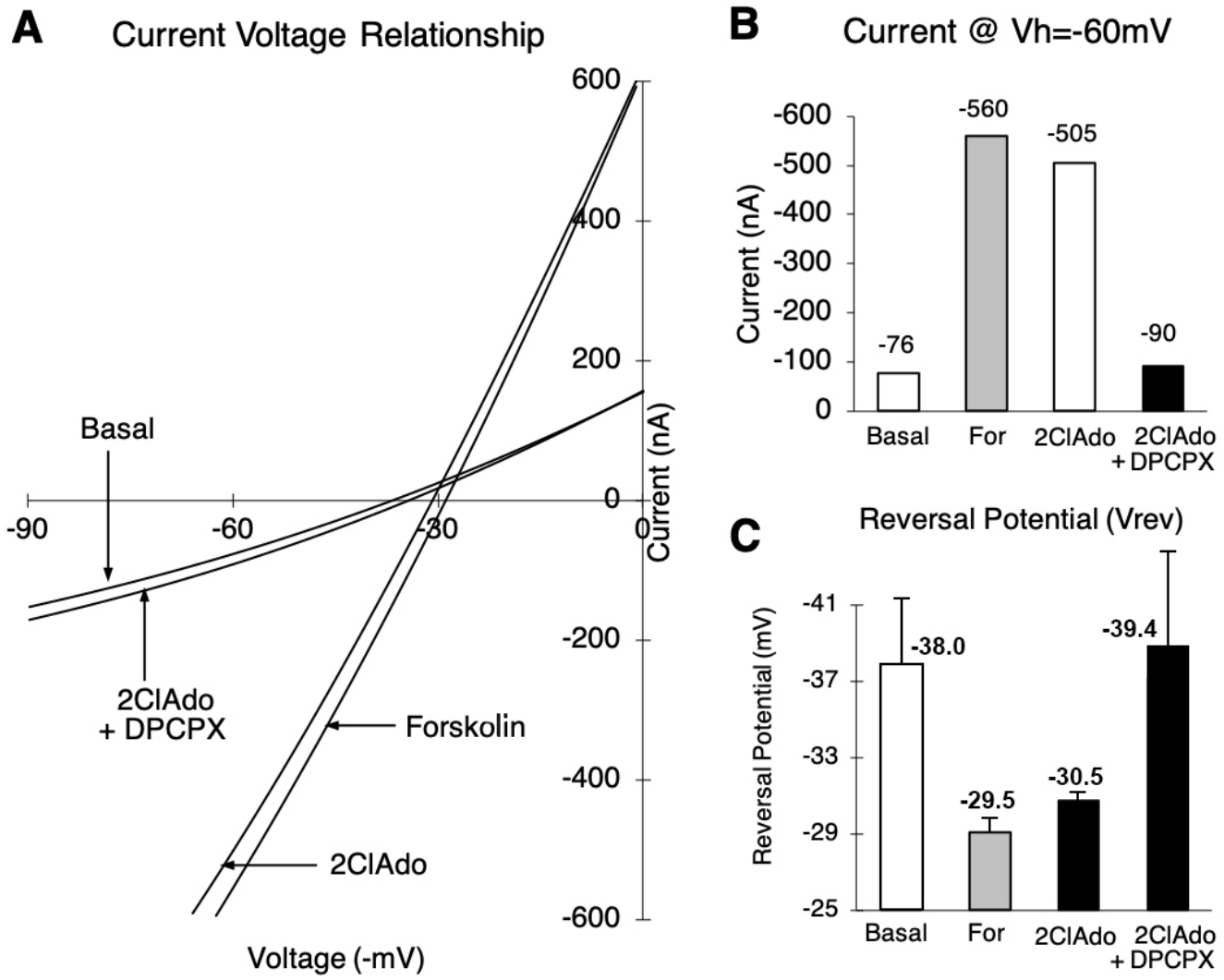

Figure 2. Current-Voltage (I-V) relationship illustrating the effects of forskolin, 2-chloroadenosine (a deaminase-resistant form of adenosine) and 2-chloroadenosine & DPCPX (a known adenosine receptor antagonist) in a representative oocyte co-expressing the shark A_0 receptor and human CFTR Cl^- channel. Panel A: selected single I-V plots for basal, forskolin, 2ClAdo and 2ClAdo+DPCPX. Panel B: Corresponding total oocyte current at -60 mV clamping voltage for the plots in panel A. Panel C: Reversal potentials (mean ± SD) were obtained for basal (-38.0 ± 3.8, n=5), forskolin ("For", -29.5 ± 0.74, n=3), 2ClAdo (-30.5 ± 0.28, n=4) and 2ClAdo+DPCPX (-39.4 ± 4.8, n=3).

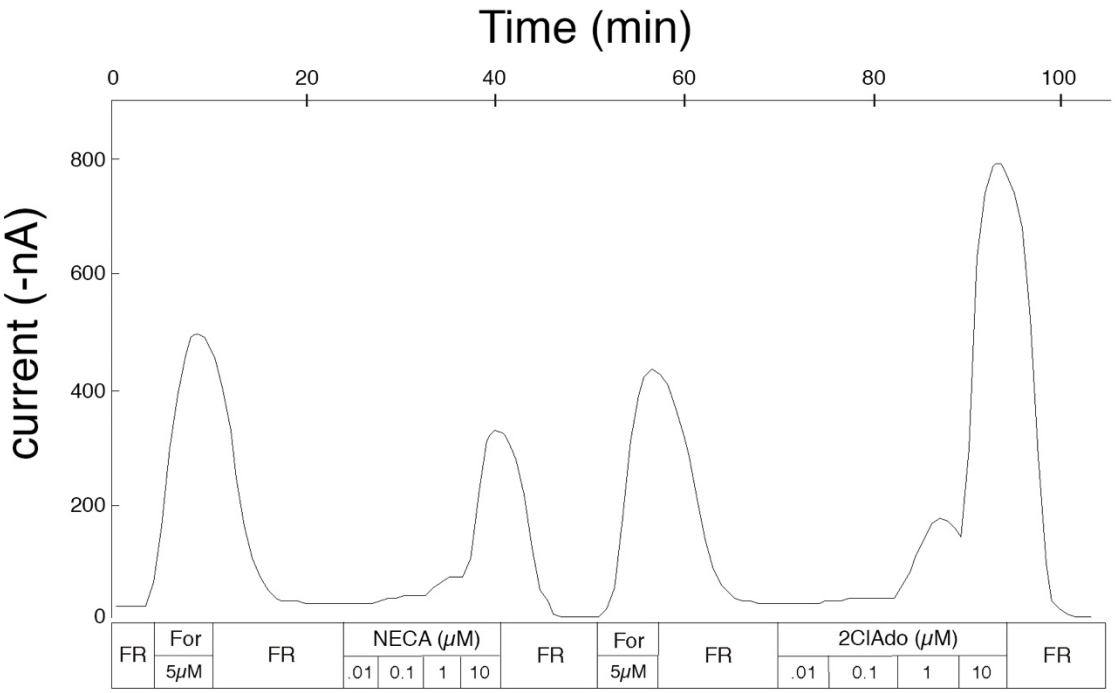

Figure 3. Representative tracing for the determination of the concentration response profile for the shark A_0 adenosine receptor. A total of four oocytes were used for the determination of the concentration response reported in the main text. Three oocytes, including results from one representative shown in the figure, were exposed to multiple sequences of incremental concentrations of NECA, 2-chloroadenosine and R-PIA (not shown in the figure), while the fourth was used for the study of R-PIA exclusively. Following any stimulation of the oocytes (with For or adenosine analogs), oocytes were returned to basal levels by perifusion with FR.

522
523

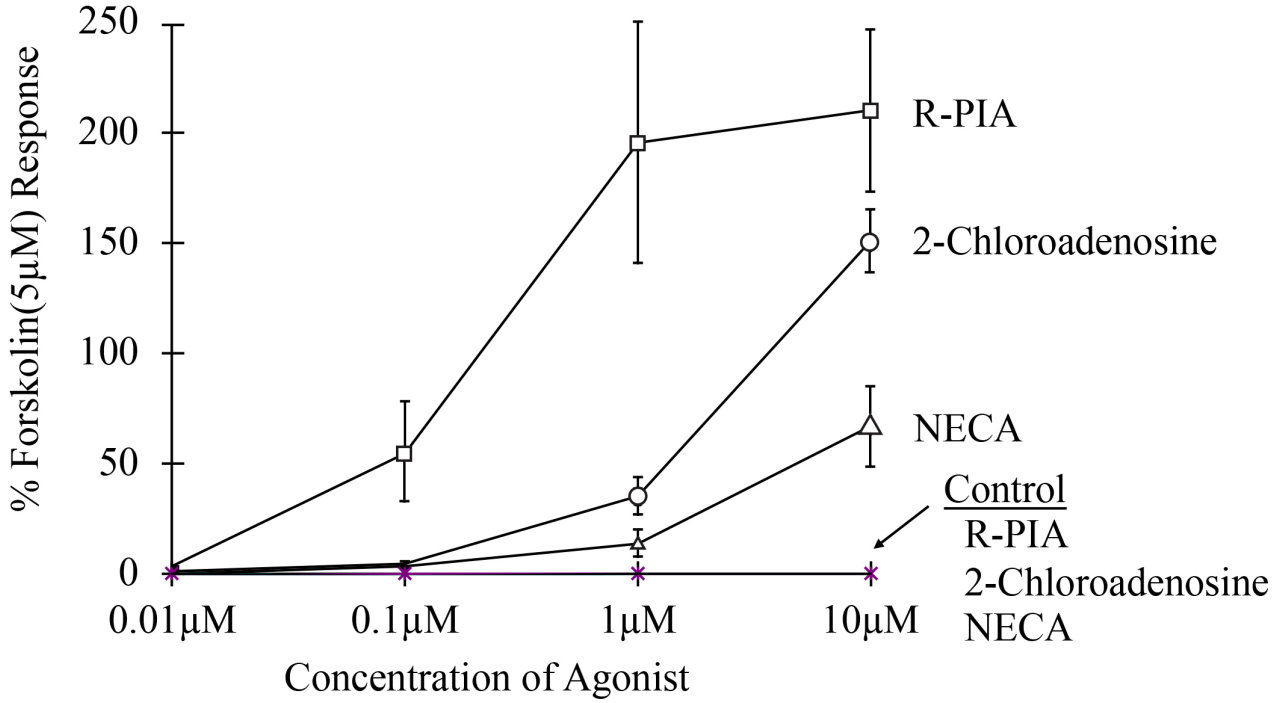

524

525 **Figure 4**. Concentration response of the shark A_0 adenosine receptor in both A_0- and CFTR- co-injected
526 oocytes as well as CFTR only-injected oocytes (labeled "Control" in the figure). The controls were conducted
527 in three oocytes, with each agonist tested in each of the three oocytes (see asterisks (*) on the x-axis). The
528 experimental group was tested in four oocytes (NECA, n=3; 2-chloroadenosine, n=3; R-PIA, n=6; and are
529 highlighted in open squares, open triangles and open triangles, respectively). The y-axis is expressed in terms
530 of the percent response to 5 μM forskolin in total oocyte current (nA).

531

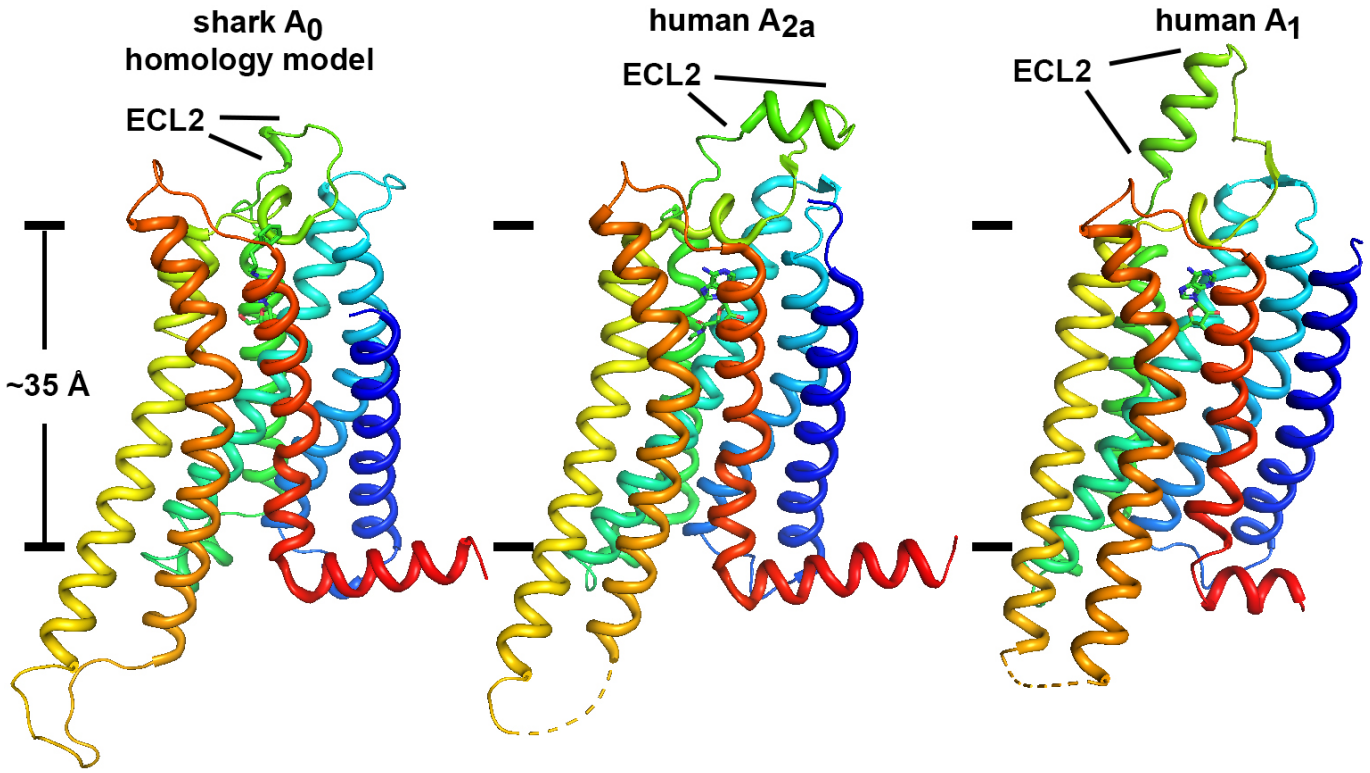

532
533
534 **Figure 5**. Overall view of the shark A_0 homology model compared to human A_{2a} and A_1 receptors (PDB
535 codes 2ydv and 6d9h). The approximate position of the hydrophobic stretch of the lipid bilayer is depicted
536 with lines separated by ~ 35 Å using conserved aromatic side chains as fiducials (27). A striking feature
537 of shark A_0 compared to the more specialized ADORs is an abbreviated extracellular loop 2 (ECL2,
538 labeled) and the relatively low profile that the A_0 receptor presents to the extracellular milieu. Multiple
539 sequence alignment of all known- and putative receptor orthologs (supplementary figs. S9 and S10)
540 reveals that an abbreviated ECL2 appears to be unique feature of ancestral ADORs.
541
542

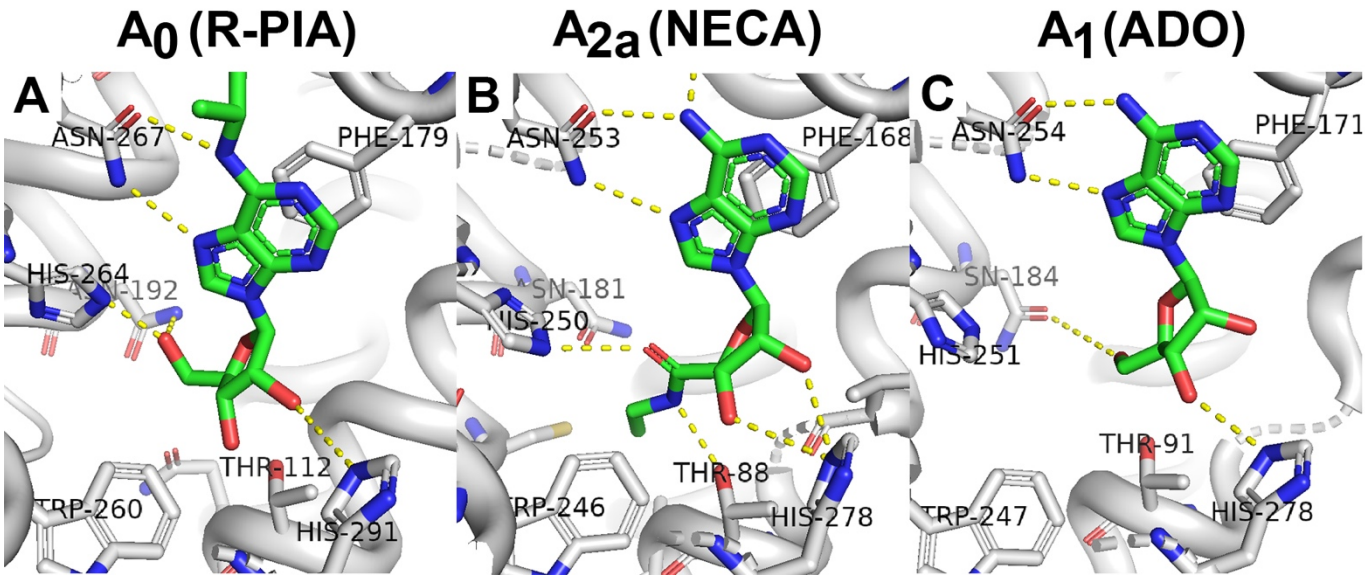

Figure 6. Binding pockets for adenosine and adenosine agonists. Panel A shows a potential binding mode of R-phenyl-isopropyl adenosine (R-PIA) as it appears in our refined homology model of the shark A_0 receptor. The purpose is not to highlight precise interactions, bonds or geometry, but to indicate that the major known adenosine-binding ligands are conserved in the shark A_0 ancestor receptor and are well positioned to potentially interact with ligands. For comparison, the location of N-ethyl-carboxyl adenosine (NECA) binding in the 2.6 Å x-ray structure of human A_{2a} receptor (PDB code 2ydv) is shown in panel B. Panel C shows the location of adenosine (ADO) binding in the 3.6 Å cryo-EM structure of the human A_1 receptor (PDB code 6d9h).

555 **References**

556 1. Burnstock, G. (1978) *A basis for distinguishing two types of purinergic receptor.*, Raven Press,
557 New York
558 2. Olah, M. E. (1997) Identification of A2a adenosine receptor domains involved in selective
559 coupling to Gs. Analysis of chimeric A1/A2a adenosine receptors. *J Biol Chem* **272**, 337-344
560 3. Sweeney, M. I., and Dolphin, A. C. (1995) Adenosine A1 agonists and the Ca2+ channel agonist
561 bay K 8644 produce a synergistic stimulation of the GTPase activity of Go in rat frontal cortical
562 membranes. *J Neurochem* **64**, 2034-2042
563 4. Palmer, T. M., and Stiles, G. L. (1995) Adenosine receptors. *Neuropharmacology* **34**, 683-694
564 5. Jockers, R., Linder, M. E., Hohenegger, M., Nanoff, C., Bertin, B., Strosberg, A. D., Marullo, S.,
565 and Freissmuth, M. (1994) Species difference in the G protein selectivity of the human and
566 bovine A1-adenosine receptor. *J Biol Chem* **269**, 32077-32084
567 6. Marala, R. B., and Mustafa, S. J. (1993) Direct evidence for the coupling of A2-adenosine
568 receptor to stimulatory guanine nucleotide-binding-protein in bovine brain striatum. *J*
569 *Pharmacol Exp Ther* **266**, 294-300
570 7. Freholm, B. B. e. a. (1994) Nomenclature and Classification of Purinoceptors. *Pharmacological*
571 *Reviews* **46**, 143-156
572 8. Burns, R. F., Lu, G. H., and Pugsley, T. A. (1987) Adenosine Receptor Subtypes: Binding Studies.
573 in *Topics and Prespectives in Adenosine Research*, Springer-Verlag, Berlin, Heidelberg. pp 59-73
574 9. Kelley, G., Aassar, O., and Forrest, J. J. (1991) Endogenous adenosine is an autocoid feedback
575 inhibitor f chloride transport in the shark rectal gland. *Journal of clinical investigation* **88**, 1933-
576 1939
577 10. Forrest, J. N. J. (1996) Cellular and molecular biology of chloride secretion in the shark rectal
578 gland: regulation by adenosine receptors. [Review]. *Kidney International* **49(6)**, 1557-1562
579 11. Forrest, J. N., Jr., Aller, S. G., Wood, S. J., Ratner, M. A., Forrest, J. K., and Kelley, G. G. (1997)
580 Cadmium disrupts the signal transduction pathway of both inhibitory and stimulatory receptors
581 regulating chloride secretion in the shark rectal gland. *J Exp Zool* **279**, 530-536
582 12. Marshall, J., Martin, K., Picciotto, M., HOCkfield, S., Nairn, A., and Kaczmarek, L. (1991)
583 Identification and localization of a dogfish homolog of human cyctic fibrosis transmembrance
584 conductance regulator. *The journal of biological chemistry* **266**, 22749-22754
585 13. Wakisaka, N., Miyasaka, N., Koide, T., Masuda, M., Hiraki-Kajiyama, T., and Yoshihara, Y. (2017)
586 An Adenosine Receptor for Olfaction in Fish. *Curr Biol* **27**, 1437-1447 e1434
587 14. Thompson, J. D., Higgins, D. G., and Gibson, T. J. (1994) CLUSTAL W: improving the sensitivity of
588 progressive multiple sequence alignment through sequence weighting, position-specific gap
589 penalties and weight matrix choice. *Nucleic Acids Res* **22**, 4673-4680
590 15. Madeira, F., Park, Y. M., Lee, J., Buso, N., Gur, T., Madhusoodanan, N., Basutkar, P., Tivey, A. R.
591 N., Potter, S. C., Finn, R. D., and Lopez, R. (2019) The EMBL-EBI search and sequence analysis
592 tools APIs in 2019. *Nucleic Acids Res* **47**, W636-W641
593 16. Rice, P., Longden, I., and Bleasby, A. (2000) EMBOSS: the European Molecular Biology Open
594 Software Suite. *Trends Genet* **16**, 276-277
595 17. Nordstrom, K. J., Sallman Almen, M., Edstam, M. M., Fredriksson, R., and Schioth, H. B. (2011)
596 Independent HHsearch, Needleman--Wunsch-based, and motif analyses reveal the overall
597 hierarchy for most of the G protein-coupled receptor families. *Mol Biol Evol* **28**, 2471-2480
598 18. Kumar, S., Stecher, G., and Tamura, K. (2016) MEGA7: Molecular Evolutionary Genetics Analysis
599 Version 7.0 for Bigger Datasets. *Mol Biol Evol* **33**, 1870-1874

600 19. Lebon, G., Warne, T., Edwards, P. C., Bennett, K., Langmead, C. J., Leslie, A. G., and Tate, C. G.
601 (2011) Agonist-bound adenosine A2A receptor structures reveal common features of GPCR
602 activation. *Nature* **474**, 521-525
603 20. Draper-Joyce, C. J., Khoshouei, M., Thal, D. M., Liang, Y. L., Nguyen, A. T. N., Furness, S. G. B.,
604 Venugopal, H., Baltos, J. A., Plitzko, J. M., Danev, R., Baumeister, W., May, L. T., Wootten, D.,
605 Sexton, P. M., Glukhova, A., and Christopoulos, A. (2018) Structure of the adenosine-bound
606 human adenosine A1 receptor-Gi complex. *Nature* **558**, 559-563
607 21. Garcia-Nafria, J., Lee, Y., Bai, X., Carpenter, B., and Tate, C. G. (2018) Cryo-EM structure of the
608 adenosine A2A receptor coupled to an engineered heterotrimeric G protein. *Elife* **7**
609 22. Lebon, G., Edwards, P. C., Leslie, A. G., and Tate, C. G. (2015) Molecular Determinants of
610 CGS21680 Binding to the Human Adenosine A2A Receptor. *Mol Pharmacol* **87**, 907-915
611 23. Sayers, E. (2017) Database Resources of the National Center for biotechnology Information.
612 *Nucleic Acids Res* **45**, D12-D17
613 24. Emsley, P., Lohkamp, B., Scott, W. G., and Cowtan, K. (2010) Features and development of Coot.
614 *Acta Crystallogr D Biol Crystallogr* **66**, 486-501
615 25. Adams, P. D., Afonine, P. V., Bunkoczi, G., Chen, V. B., Davis, I. W., Echols, N., Headd, J. J., Hung,
616 L. W., Kapral, G. J., Grosse-Kunstleve, R. W., McCoy, A. J., Moriarty, N. W., Oeffner, R., Read, R.
617 J., Richardson, D. C., Richardson, J. S., Terwilliger, T. C., and Zwart, P. H. (2010) PHENIX: a
618 comprehensive Python-based system for macromolecular structure solution. *Acta Crystallogr D*
619 *Biol Crystallogr* **66**, 213-221
620 26. Weininger, D. (1988) SMILES, a chemical language and information system. *J Chem Inform*
621 *Computer Sci* **28**, 31-36
622 27. de Planque, M. R., Kruijtzer, J. A., Liskamp, R. M., Marsh, D., Greathouse, D. V., Koeppe, R. E.,
623 2nd, de Kruijff, B., and Killian, J. A. (1999) Different membrane anchoring positions of
624 tryptophan and lysine in synthetic transmembrane alpha-helical peptides. *J Biol Chem* **274**,
625 20839-20846
626 28. Devor, D. C., Forrest, J. N., Jr., Suggs, W. K., and Frizzell, R. A. (1995) cAMP-activated Cl-
627 channels in primary cultures of spiny dogfish (Squalus acanthias) rectal gland. *Am J Physiol* **268**,
628 C70-79
629 29. Xu, F., Wu, H., Katritch, V., Han, G. W., Jacobson, K. A., Gao, Z. G., Cherezov, V., and Stevens, R.
630 C. (2011) Structure of an agonist-bound human A2A adenosine receptor. *Science* **332**, 322-327
631 30. Birnbaum, A. K., Wotta, D. R., Law, P. Y., and Wilcox, G. L. (1995) Functional expression of
632 adrenergic and opioid receptors in Xenopus oocytes: interaction between alpha 2- and beta 2-
633 adrenergic receptors. *Brain Res Mol Brain Res* **28**, 72-80
634 31. Uezono, Y., Bradley, J., Min, C., McCarty, N. A., Quick, M., Riordan, J. R., Chavkin, C., Zinn, K.,
635 Lester, H. A., and Davidson, N. (1993) Receptors that couple to 2 classes of G proteins increase
636 cAMP and activate CFTR expressed in Xenopus oocytes. *Receptors Channels* **1**, 233-241
637 32. Forrest, J. N., Jr. (2016) The Shark Rectal Gland Model: A Champion of Receptor Mediated
638 Chloride Secretion through Cftr. *Trans Am Clin Climatol Assoc* **127**, 162-175
639 33. Clancy, J. P., Ruiz, F. E., and Sorscher, E. J. (1999) Adenosine and its nucleotides activate wild-
640 type and R117H CFTR through an A2B receptor-coupled pathway. *Am J Physiol* **276**, C361-369
641 34. Kelley, G. G., Poeschla, E. M., Barron, H. V., and Forrest, J. N., Jr. (1990) A1 adenosine receptors
642 inhibit chloride transport in the shark rectal gland. Dissociation of inhibition and cyclic AMP. *J*
643 *Clin Invest* **85**, 1629-1636
644 35. Saitou, N., and Nei, M. (1987) The neighbor-joining method: a new method for reconstructing
645 phylogenetic trees. *Mol Biol Evol* **4**, 406-425

646 36. Zuckerkandl, E. a. P., L. (1965) Evolutionary divergence and convergence in proteins. in *Evolving*
647 *Genes and Proteins*, Academic Press, New York. pp 97-166
648